

AD-A184 770

EROSIVE BURNING STUDY OF STICK PROPELLANTS(U)  
PENNSYLVANIA STATE UNIV UNIVERSITY PARK DEPT OF  
MECHANICAL EN. W H HSIEH ET AL 06 AUG 87

1/1

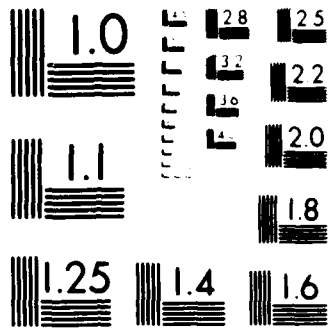
UNCLASSIFIED

PSU-ME-P-86/87-0041 ARO-20007 8-EG

F/G 19/1

NL

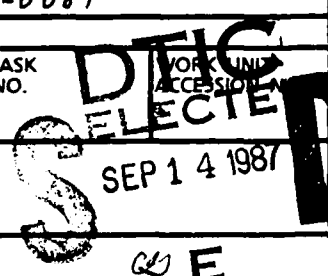




MICROCOPY RESOLUTION TEST CHART  
NATIONAL BUREAU OF STANDARDS-1963-A

AD-A184 770

REPORT DOCUMENTATION PAGE

2a. SECURITY CLASSIFICATION AUTHORITY		1b. RESTRICTIVE MARKINGS	
2b. DECLASSIFICATION/DOWNGRADING SCHEDULE		3. DISTRIBUTION/AVAILABILITY OF REPORT Approved for public release; distribution unlimited.	
4. PERFORMING ORGANIZATION REPORT NUMBER(S) PSU-ME-P-86/87- 0041		5. MONITORING ORGANIZATION REPORT NUMBER(S) ARU 20007.8-EG	
6a. NAME OF PERFORMING ORGANIZATION Penn State University	6b. OFFICE SYMBOL (if applicable)	7a. NAME OF MONITORING ORGANIZATION U. S. Army Research Office	
6c. ADDRESS (City, State, and ZIP Code) 312 Mechanical Engineering Building University Park, PA 16802 USA		7b. ADDRESS (City, State, and ZIP Code) P. O. Box 12211 Research Triangle Park, NC 27709-2211	
8a. NAME OF FUNDING/SPONSORING ORGANIZATION U. S. Army Research Office	8b. OFFICE SYMBOL (if applicable)	9. PROCUREMENT INSTRUMENT IDENTIFICATION NUMBER DAA629-83-K-0081	
8c. ADDRESS (City, State, and ZIP Code) P. O. Box 12211 Research Triangle Park, NC 27709-2211		10. SOURCE OF FUNDING NUMBERS	
		PROGRAM ELEMENT NO.	TASK NO.
11 TITLE (Include Security Classification) "Erosive Burning Study of Stick Propellants"		 <p>SEP 14 1987</p>	
12 PERSONAL AUTHOR(S) W. H. Hsieh, J. M. Char, C. Zanotti, and K. K. Kuo			
13a. TYPE OF REPORT Interim	13b. TIME COVERED FROM _____ TO _____	14. DATE OF REPORT (Year, Month, Day) 1987, August 6	15. PAGE COUNT 9
16. SUPPLEMENTARY NOTATION The view, opinions and/or findings contained in this report are those of the author(s) and should not be construed as an official Department of the Army position, policy, or decision, unless so designated by other documentation.			
17. COSATI CODES		18. SUBJECT TERMS (Continue on reverse if necessary and identify by block number)	
FIELD	GROUP	Erosive Burning; Stick Propellants; Turbulent Mixing; X-ray Radiography; Nonintrusive Measurements; NOSOL-363 Propellant Strand-burning Rates.	
19 ABSTRACT (Continue on reverse if necessary and identify by block number) A theoretical model was solved numerically for simulating erosive-burning processes occurring inside the center perforation of an unslotted NOSOL-363 stick propellant. Results show that the erosive-burning phenomenon is caused by the enhanced heat feedback from the gas phase to solid phase resulting from the combined effect of increased turbulent mixing and reduction in flame stand-off distance from the burning surface. The real-time X-ray radiography system was demonstrated to be a powerful and reliable tool for nonintrusive measurements of instantaneous burning rates. A model was validated by experimental data in terms of time variation of internal diameter distributions. Thermal wave structures of NOSOL-363 stick propellants under erosive- and strand-burning conditions were measured by fine-wire thermocouples.			
20. DISTRIBUTION/AVAILABILITY OF ABSTRACT <input type="checkbox"/> UNCLASSIFIED/UNLIMITED <input type="checkbox"/> SAME AS RPT. <input type="checkbox"/> DTIC USERS		21. ABSTRACT SECURITY CLASSIFICATION Unclassified	
22a. NAME OF RESPONSIBLE INDIVIDUAL Kenneth K. Kuo		22b. TELEPHONE (Include Area Code) (814) 865-6741	22c. OFFICE SYMBOL

# AIAA'87

**AIAA-87-2032**

## **Erosive Burning Study of Stick Propellants**

W. H. Hsieh, J. M. Char, C. Zanotti, and K. K. Kuo

The Pennsylvania State University  
University Park, PA 16802

Accession For	
NTIS GRA&I	<input checked="" type="checkbox"/>
DTIC TAB	<input type="checkbox"/>
Unannounced	<input type="checkbox"/>
Justification	
By	
Distribution/	
Availability Codes	
Dist	Avail and/or Special
A-1	

QUALITY INSPECTED  
2

## **AIAA/SAE/ASME/ASEE 23rd Joint Propulsion Conference**

June 29-July 2, 1987/San Diego, California

For permission to copy or republish, contact the American Institute of Aeronautics and Astronautics  
1633 Broadway, New York, NY 10019

## EROSIVE-BURNING STUDY OF STICK PROPELLANTS\*

W. H. Hsieh,<sup>1</sup> J. M. Char,<sup>2</sup> C. Zanotti,<sup>3</sup>  
and K. K. Kuo<sup>4</sup>

Department of Mechanical Engineering  
The Pennsylvania State University  
University Park, PA 16802

### ABSTRACT

A theoretical model was solved numerically for simulating erosive-burning processes occurring inside the center perforation of an unslotted NOSOL-363 stick propellant. Results show that the erosive-burning phenomenon is caused by the enhanced heat feedback from the gas phase to solid phase resulting from the combined effect of increased turbulent mixing and reduction in flame stand-off distance from the burning surface. The real-time X-ray radiography system was demonstrated to be a powerful and reliable tool for nonintrusive measurements of instantaneous burning rates. A model was validated by experimental data in terms of time variation of internal diameter distributions. Thermal wave structures of NOSOL-363 stick propellants under erosive- and strand-burning conditions were measured by fine-wire thermocouples.

### INTRODUCTION

There has been increasing interest in the use of single-perforated stick propellants in large-caliber gun systems. In order to accurately analyze and predict the interior ballistic performance of large-caliber gun systems using stick propellants, the erosive- and strand-burning characteristics of the propellants must be determined. Stick-propellant grains recovered from test firings using simulated guns<sup>1,2</sup> showed coning phenomena of the internal surfaces on both ends. This suggests the importance of erosive burning in the combustion of stick-propellant bundles.

In the past, no attempt had been made to study thermal wave structures (subsurface temperature profiles, burning surface temperatures, dark zone lengths, characteristic times, etc.) of NOSOL-363 stick propellants. Nor has the strand burning rate been measured at low pressures (less than 69 atm). Although the burning-rate exponent for NOSOL-363 stick propellants was found to be 0.965 at high pressures<sup>3</sup> (370-2220 atm), this value may not be

suitable for low-pressure conditions; the combustion mechanism of NOSOL-363 stick propellants would vary at different pressure ranges and result in different values of burning-rate exponents.

Erosive burning of various solid propellants was studied extensively under different cross-flow situations.<sup>4</sup> However, due to the limitation of past measurement techniques and hostile experimental conditions, the instantaneous burning surface locations and erosive-burning rates along the internal perforation of a cylindrical propellant grain could not be easily determined. Recently, Hsieh et al.<sup>5</sup> successfully demonstrated the feasibility of using real-time X-ray radiography to measure erosive-burning rates of a center-perforated cylindrical stick-propellant grain. A comprehensive theoretical model was also formulated by Hsieh and Kuo<sup>5,6</sup> to take into account the strong interaction of turbulence and combustion under erosive-burning conditions.

The objectives of this study are: 1) to use real-time X-ray radiography to measure instantaneous burning surface locations along the center perforation of NOSOL-363 stick-propellant grain; 2) to validate the theoretical model<sup>5,6</sup> by experimental data; 3) to study the erosive-burning characteristics of the stick propellants using the theoretical model developed by the authors; 4) to determine the strand burning characteristics of the propellants at pressures lower than 69 atm; 5) to study the thermal wave structures of NOSOL-363 stick propellants under cross-flow (erosive burning) and/or no cross-flow (strand burning) conditions; 6) to deduce various important thermochemical properties (such as burning surface temperature as a function of pressure, thermal diffusivity, activation energy and preexponential factor for Arrhenius pyrolysis law, burning-rate exponent  $n$  and constant  $a$  for Saint Robert's burning rate law); and 7) to examine the differences in combustion characteristics between strand- and erosive-burning conditions in order to gain a deeper understanding of erosive-burning phenomena.

### METHOD OF APPROACH

#### Experimental Approach

#### 1. Measurement of Instantaneous Burning Surface Locations along the Center Perforation of an Unslotted Cylindrical Stick-Propellant Grain

In this study, a test rig using a center-perforated cylindrical propellant grain with large web thickness (~1.0 cm) was designed and constructed<sup>5</sup> to observe erosive-burning phenomena and to obtain a data base for model validation (see Fig. 1). Instantaneous locations of internal burning surface of a cylindrical stick-propellant grain were determined by the use of real-time X-ray radiography, which consists of a constant potential continuous-wave X-ray system, an image intensifier, a Spin Physics high-speed digitize

\*This work represents a part of the research results obtained from the project sponsored by the Engineering Sciences Division of the Army Research Office under Contract No. DAAK29-83-K-0081. The technical program manager is Dr. David M. Mann. His encouragement and support is greatly appreciated. The authors would also like to thank Mr. F. Robbins of BRL for his support and arrangement of processing and shipment of propellant grains required for this investigation.

<sup>1</sup>Ph.D. Candidate, Research Assistant, Student Member of AIAA

<sup>2</sup>Ph.D. Candidate

<sup>3</sup>Visiting Research Associate, on leave from CNPM-CNR, Milan, Italy

<sup>4</sup>Distinguished Alumni Professor of Mechanical Engineering, Associate Fellow of AIAA



solid phase under a steady-state condition can be expressed in an exponential form. The characteristic time of the thermal wave in the solid propellant is determined by curve fitting the raw data of  $[T(t) - T(0)]$  versus time into an exponential form. After the burning rate  $r_b$  has been determined from recorded test images, the thermal diffusivity is calculated from Eq. (1). The characteristic thermal wave length is equal to the product of the characteristic time and burning rate. The temperature profile in the solid phase of NOSOL-363 stick propellant is a straight line plot of  $\ln(T - T_0)$  versus  $t$ . The point of departure from the straight line is taken to be the burning surface temperature.

### 3. Experimental Setup for Strand-Burning Rate Measurements

Figure 4 shows the schematic diagram of the test rig used in strand-burning rate measurements. A propellant strand was mounted vertically between two electrical terminal posts. Ignition of the propellant strand was achieved by passing electrical current through a nichrome wire which was in contact with the top surface of the propellant strand. During the test, a small amount of nitrogen gas flowed continuously from the bottom end to the top end of the chamber. The nitrogen gas flow was used to carry the combustion product gases out of the test chamber so that the windows, on both sides of the test rig, could remain clean for observing combustion phenomena and recording the instantaneous location of the burning propellant surface.

A scale was optically superimposed on the image of propellant strand by a semi-transparent mirror (Rolynd Dielectric Beam Splitter). A Panasonic VCR was used to record test images and the superimposed scale through the window at the rate of 30 frames/sec. From the scale superimposed on the test image, the length of the strand burned in a certain amount of time could be precisely measured, and the burning rate could then be determined.

The chamber pressure was measured by a Validyne pressure transducer (DP215) and a carrier demodulator (CD15) which had a frequency response of 1000 Hz. The chamber pressure was kept constant by a Skinner solenoid valve (XLB11002)

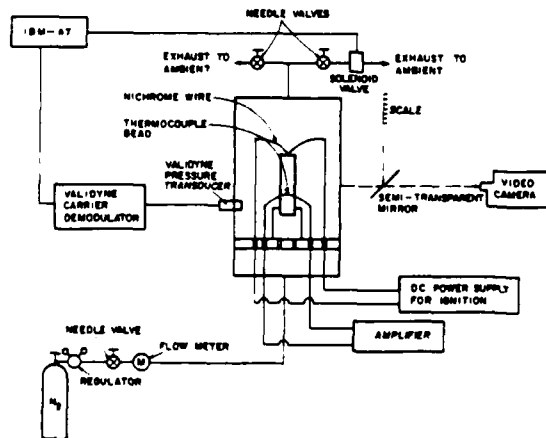


Fig. 4 Schematic Diagram of Experimental Apparatus Used in Strand-Burning Rate Test

which could be operated at the maximum rate of 10 cycles/sec. Operation of the Skinner solenoid valve was controlled by an IBM-AT personal computer. Utilizing the above-mentioned equipment and the accompanying software, pressure fluctuation of the test chamber during a test could be limited to within  $\pm 1\%$  of a preselected pressure level (1-69 atm).

Figure 5 shows the data acquisition system for recording temperature and pressure data during strand-burning tests. The voltage output of the thermocouple is amplified about 200 times by a wide-band amplifier which has a frequency response of 100 kHz. During the test, the amplified voltage output of thermocouple and pressure data were recorded in a Nicolet 4094 digital oscilloscope with Nicolet 4562 plug-in and XF-44 disk recorder. After test firing, the voltage data of thermocouple output were transferred to an IBM-AT personal computer via an RS-232 bus and were then converted to temperature data for further data reduction to determine various propellant characteristics.

### THEORETICAL APPROACH

A comprehensive theoretical model was formulated<sup>5-7</sup> and solved numerically for simulating erosive-burning processes occurring inside the perforation of a NOSOL-363 stick propellant. Both gas- and solid-phase regions of the propellant were considered in the theoretical model. A two-variable joint probability density function was adopted to take into account the interaction of gas-phase turbulence and combustion. A transient one-dimensional heat-conduction equation with consideration of subsurface radiation absorption was used to describe the thermal wave structure of the condensed phase of the propellant.

The set of gas-phase simultaneous partial differential equations was solved by the implicit, finite-difference method of Patankar and Spalding.<sup>11</sup> For the solid phase, the transient heat-conduction equation and radiation heat-flux equations were solved, using a central-difference technique, to obtain the temperature distributions in the stick propellant as a function of time. Detailed finite-difference equation and numerical procedures for both regions can be found in Refs. 12 and 13.

### DISCUSSION OF RESULTS

Figure 6 shows the comparison between the calculated radius and experimental data obtained under erosive-burning conditions. The theoretical predictions compare well with measured data at various times. Time variation of the

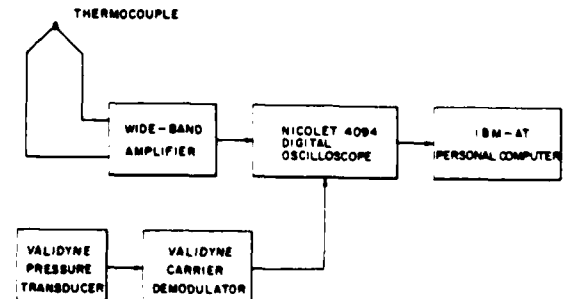


Fig. 5 Schematic Diagram of Data Acquisition System Used in Strand-Burning Tests

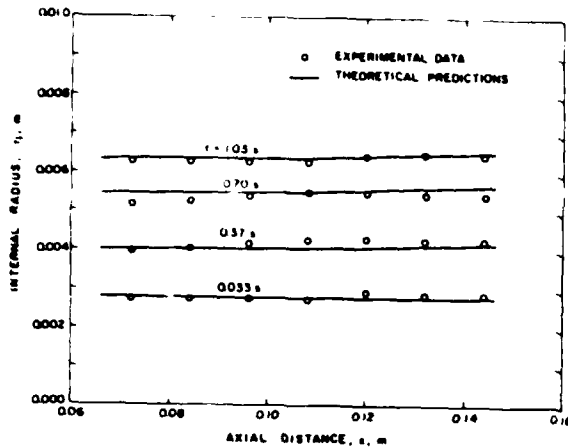


Fig. 6 Comparison Between Calculated Internal Radius and Experimental Data Obtained from Erosive-Burning Test Using Thick-Walled NOSOL-363 Stick-Propellant Grain (Test No. 24)

erosive-burning rates along the propellant grains as shown in Fig. 7. The burning rate apparently decreases as time increases; this is due to the fact that pressure and velocity are decreasing with respect to time. In the early time period ( $t < 0.37$  s), the burning rates at downstream locations are higher than those at upstream locations because of increased mass flow rate in the downstream direction. As time passes, the cross-flow velocity drops as the port area increases, and the pressure effect becomes more important. This causes the site of maximum burning to move in the upstream direction.

Figure 8 shows the calculated velocity profiles at three axial positions. The center-line velocity is increasing with  $x$ . This is caused by the mass addition and growth of boundary layer thickness along the axial direction. Due to the mass injection from the burning propellant surface, the velocity profile becomes fuller at downstream locations. These phenomena were also reported by Trainean et al.<sup>14</sup> in experimental data obtained in a cold-flow test of a nozzleless rocket motor.

The distributions of turbulent kinetic energy at different axial positions are shown in Fig. 9. As  $x$  increases, the magnitude of turbulent kinetic energy increases, and the site of maximum turbulent kinetic energy moves closer to the wall. The same trend was also reported by Yamada et al.<sup>15</sup> and Trainean et al.<sup>14</sup>

Figure 10 shows a set of distributions of mass fractions of fuel, oxidizer, and delayed reaction species of group 1 (DRI)<sup>5,7</sup> at three different axial locations. The concentration profiles of these species are quite steep near the propellant surface. This implies that a certain portion of the chemical reactions can occur very near the propellant surface. From the overall mass-fraction distributions, it is also noted that the chemical reactions away from the propellant surface are not insignificant. Therefore, the interaction of turbulence with chemical reactions is important throughout most portions of the reacting boundary layer.

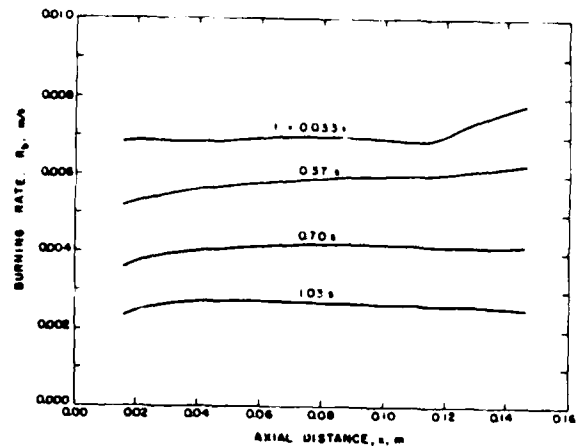


Fig. 7 Calculated Time Variation of Distributions of Erosive-Burning Rate Along the Internal Perforation of Thick-Walled NOSOL-363 Stick-Propellant Grain

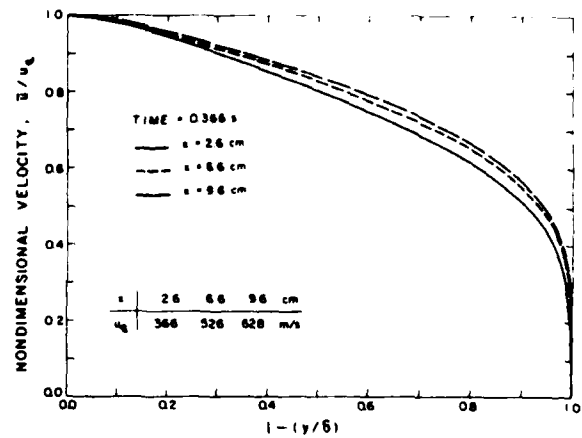


Fig. 8 Calculated Velocity Distribution in the Internal Perforation of Thick-Walled NOSOL-363 Stick-Propellant Grain

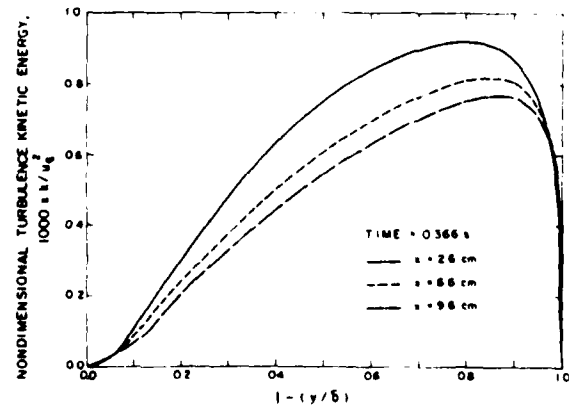


Fig. 9 Calculated Turbulence Kinetic Energy Distribution in the Internal Perforation of Thick-Walled NOSOL-363 Stick-Propellant Grain

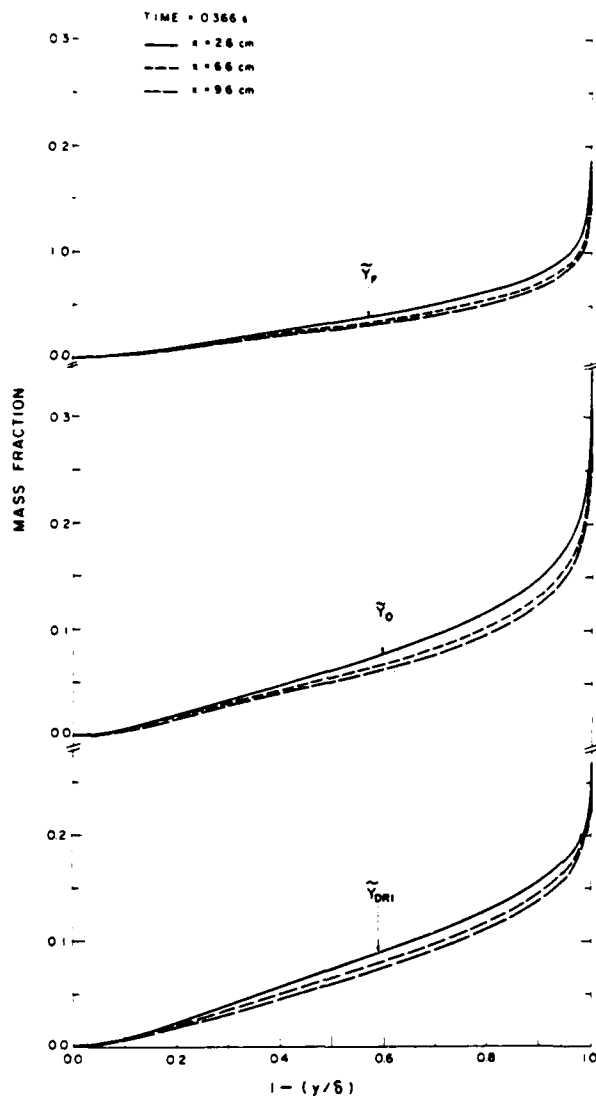


Fig. 10 Calculated Distributions of Mass Fraction of Oxidizer, Fuel, and DR1 in the Internal Perforation of Thick-Walled NOSOL-363 Stick-Propellant Grain

In the strand-burning tests, three modes of gas-phase combustion were observed, as shown in Fig. 11. At pressures lower than 7.8 atm (100 psig), no visible flame appeared in the gas phase. This mode of gas-phase combustion is known as "fizz burning."<sup>8</sup> In this mode, it was observed that relatively large-sized particles (~ 1 mm) were coming off sporadically from the burning surface of the propellant. At pressures between 7.8 and 21.4 atm (100 and 300 psig), bright, unsteady yellowish flames were observed. The visible flames were not stationary, but moved around the propellant surface in upward, downward, and sidewise directions. Also, there are several flamelets attached to the propellant surface. The attachment zone is relatively small in comparison with the sample burning surface area. In this study, this mode of combustion is called "unsteady flame." At pressures higher than 21.4 atm (300 psig), the flame is clearly visible and

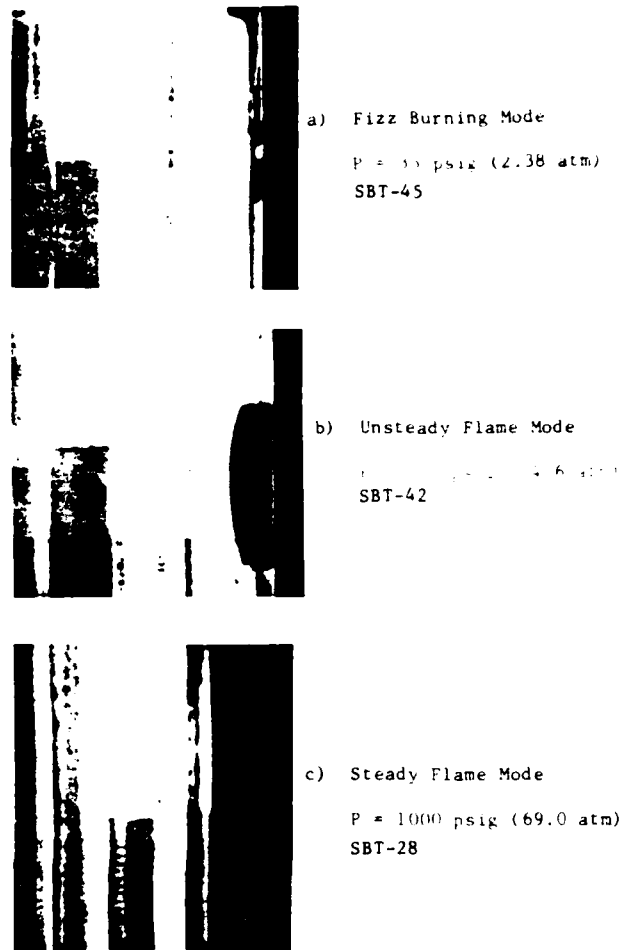


Fig. 11 Three Different Modes in the Burning of NOSOL-363 Stick Propellants

quite steady. This burning with steady luminous flame is called "steady flame mode;" it is also referred to by Kubota et al.<sup>10</sup> as "flame burning."

The observed luminous flame stand-off distance from the propellant surface decreases as pressure increases. The phenomenon of reduction in flame stand-off distance as pressure increases was first observed by Crawford and Hugget.<sup>16</sup> They measured the distance between the burning surface and the luminous flame position for pressures between 20 and 30 atm, and found that the distance was inversely proportional to the cube of the pressure. In this study, it was observed that the flame stand-off distance for NOSOL-363 stick propellants changed from 1.5 to 0.8 mm as pressure increased from 35 to 48.6 atm.

The measured strand-burning rate versus ambient pressure is plotted in Fig. 12. Each data point represents the average value of 4 to 13 measured burning rates. The maximum error is close to 5%, as shown in Fig. 12. Guided by the pressure boundary between the steady-flame mode and the unsteady-flame mode of the gas-phase reaction zone structure, the point of the slope break at 2.17 MPa (300 psig) was selected. Consequently, the burning rate data can be easily separated into two regions separated by the above slope break points. The burning-rate exponents and coefficients for the two different regions are

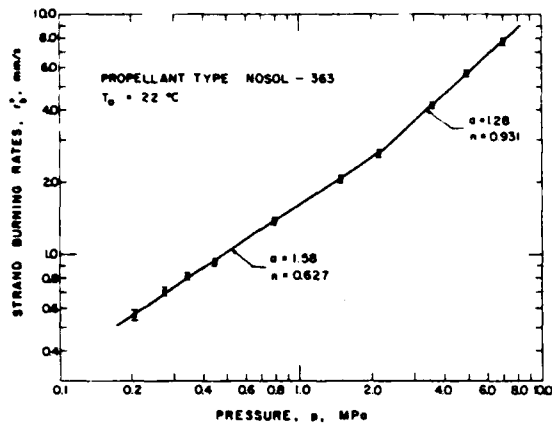


Fig. 12 Strand-Burning Rates of NOSOL-363 Stick Propellants at Various Pressures

marked on these line segments. Such a slope break has been observed for double-base homogeneous propellants.<sup>17</sup> The slope break is essentially caused by the change of the combustion mechanism and the rate of heat feedback to the propellant surface.

Figure 13 shows a typical thermal wave structure of a NOSOL-363 stick propellant. In this figure, the following characteristic zones are identified.

- Zone I is a condensed-phase zone which includes an inert heating region and a subsurface reaction region. The condensed-phase zone ends at the burning surface temperature of 320-540°C at different pressures.
- Zone II is defined as the fizz zone, which extends from the burning surface to the region at which the temperature gradient becomes small. The thickness of the zone is in the order of 80 to 300  $\mu\text{m}$  depending upon the pressure field.
- Zone III is defined as the dark zone, which extends from the end of the fizz zone to the point at which the temperature starts to increase drastically.
- Zone IV is the luminous flame zone, which extends from the point of rapidly increasing temperature. This region is indicated by bright yellowish flames in Fig. 11.

Thickness of the fizz zone depends on the chemical reaction rate of the gaseous species evolved from the burning surface. The chemical reaction rate depends on the pressure; the rate increases with increasing pressure. Therefore, the thickness of the fizz zone generally decreases as pressure increases, resulting in an increased temperature gradient and heat feedback from the gas phase to the condensed phase.

In the dark zone (i.e., Zone III), the temperature gradient is very small; this indicates slow chemical reaction. The peak temperature of the dark zone varies from 1000°C at 3.4 atm (35 psig) to 1200°C at 14.6 atm (200 psig). It increases to 1300°C at 35 atm (500 psig), and to

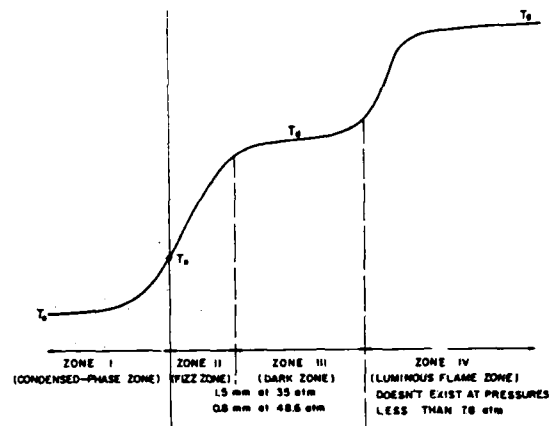


Fig. 13 Schematic Diagram of the Thermal Wave Structure of a NOSOL-363 Stick Propellant Burning Under No-Cross Flow Condition

approximately 1500°C at 48.6 atm (700psig). Further increase in pressure will eventually result in the collapse of the dark zone but will bring about only a slight increase in maximum temperature in the dark zone.

The pressure dependence of the measured burning propellant surface temperature is shown in Fig. 14. It is evident that the burning-surface temperature increases with pressure. According to Arrhenius law, the relation between strand-burning rate and burning-surface temperature can be written as:

$$r_b^0 = A_s \exp [-E_{a,s} / (R_u T_s)] \quad (2)$$

where  $E_{a,s}$  and  $A_s$  are the activation energy and pre-exponential factor.

In order to examine the relation between burning-surface temperatures and strand-burning rates of NOSOL-363 stick propellants,  $r_b^0$  versus  $1/T_s$  is plotted in Fig. 15. Using least-square nonlinear regression analysis, it is found that the  $E_{a,s}$  is 8.13 kcal/mole for pressures ranging from 3.4 to 21.4 atm (35 psig to 300 psig), and that the activation energy is 14.8 kcal/mole at pressures between 21.4 and 69.02 atm (300 and 1,000 psig).

Several important properties of NOSOL-363 stick propellants can be deduced from temperature profile in the condensed phase. The thermal diffusivity of the NOSOL-363 propellant, deduced from the condensed-phase temperature profile, is independent of the ambient pressure, as shown in Fig. 16. The characteristic time and characteristic length of NOSOL-363 stick propellants versus pressure are also plotted in Fig. 16. The slope breaks for both curves at 21.4 atm (300 psig) correspond to the change of combustion mechanism from unsteady-flame mode to the steady-flame mode. Based upon the fact that the characteristic time of the solid propellant being much larger than that of the thermocouple used in this study, it is evident that sizes of thermocouple wires are small enough to measure temperature profiles accurately.

A set of data obtained under erosive-burning conditions is shown in Figs. 17a and 17b. In Fig. 17a, the instantaneous internal diameter of the propellant grain and total regression rate at an

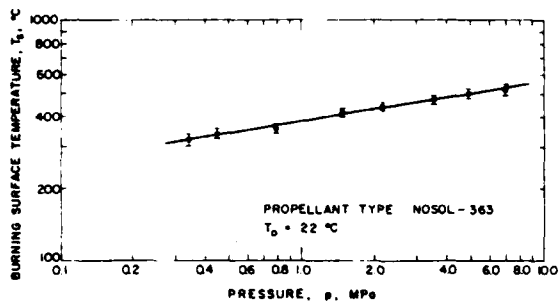


Fig. 14 Variation of Burning Surface Temperature as a Function of Pressure

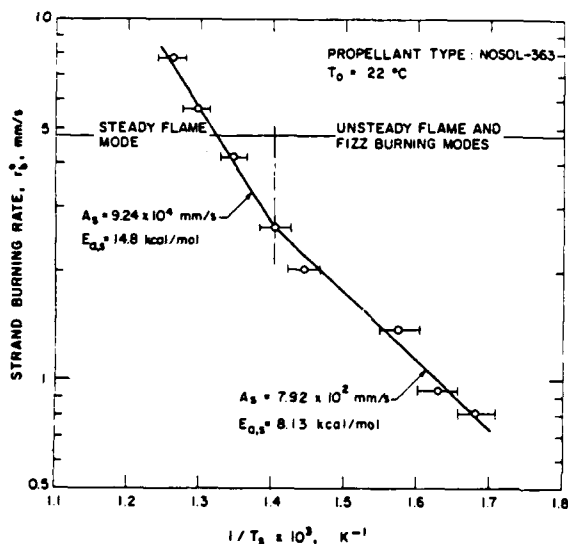


Fig. 15 Relation Between Strand-Burning Rates and Burning Surface Temperatures

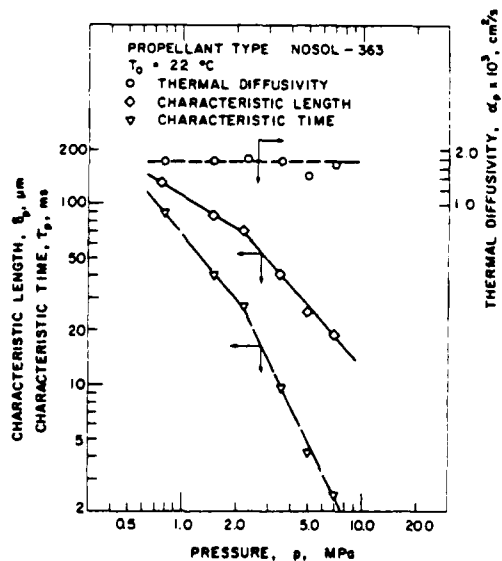


Fig. 16 Variation of Thermal Diffusivity, Characteristic Time and Characteristic Length of the NOSOL-363 Stick Propellant as a Function of Pressure

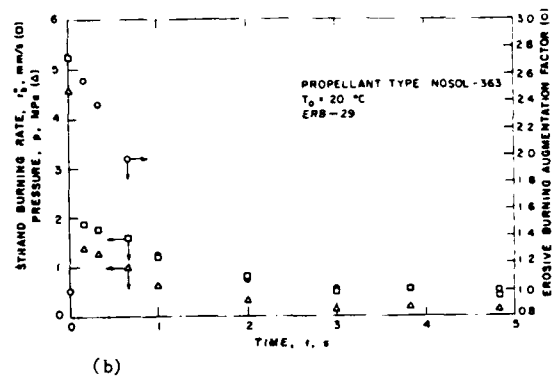
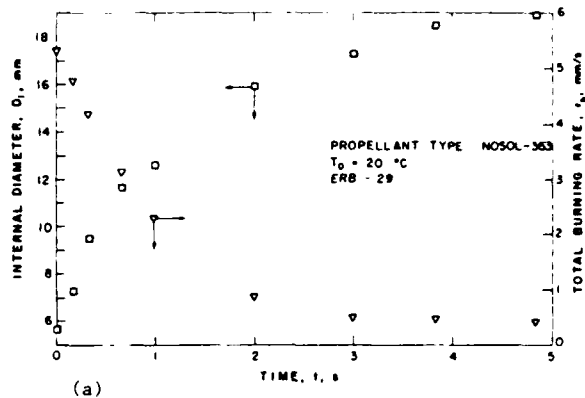


Fig. 17 Time Variations of the Internal Diameter, the Total Burning Rate, the Static Pressure, the Strand Burning Rate, and the Erosive-Burning Augmentation Factor Obtained from an Erosive-Burning Test (ERB-29)

axial station (where a fine-wire thermocouple was embedded) are plotted with respect to time. The instantaneous internal diameter variation was deduced from the real-time X-ray radiography image, and the total burning rate was determined from the differentiation of the polynomial which fits the curve of internal diameter variation. It is quite evident that the burning rate decreases rapidly during the initial time interval and remains relatively constant after 3 seconds.

In order to determine the erosive-burning augmentation factor, the pressure distribution inside the propellant grain must be known. An identical test run with multiple pressure gauges inserted at five different locations was conducted to obtain the relative relationship between the P-t traces measured by gauges located along the propellant grain and those at the two ends. For pressure gauge ports drilled through the propellant gain, flame retardant grease was applied to the port surfaces to prevent additional mass injection due to the burning of any extra propellant surfaces. The pressure-time trace corresponding to the fine-wire thermocouple station is shown in Fig. 17b. The absolute pressure level at a time period beyond 3 seconds is set equal to the strand-burner pressure giving the measured burning rate. The rest of the P-t trace, obtained from interpolation of the pressure gauge, records at both upstream and downstream

ranges, and is shifted accordingly if an adjustment is necessary. Following this procedure, the erosive-burning augmentation factor near the end of the run is set equal to unity. The strand-burning rate and the burning-rate augmentation factor are also plotted in Fig. 17b. It is evident that during the initial time interval (less than 2.0 s) the erosive-burning augmentation factor is quite significant. This is in agreement with many observed burning phenomena of center perforated grains. During the initial time interval, the cross-sectioned area of the flow is small and the mass flow rate per unit area is relatively large; hence the erosive burning is more pronounced.

The above procedure is useful in determining the time variation of the erosive-burning augmentation factor. However, due to the difficulty in measuring the absolute pressure distribution inside a center-perforated grain, the absolute value of the erosive-burning augmentation factor cannot be ascertained absolutely. It is also possible that negative erosive-burning rates could be overlooked.

A temperature-time trace recorded by a fine-wire thermocouple embedded in a propellant grain burning under crossflow conditions is shown in Fig. 18. The temperature-time traces are presented in two different forms. It is interesting to note that the trace given in  $\ln(T-T_0)$  versus time exhibits nonlinear behavior. Part of this nonlinearity could be caused by the temporal pressure variations during the test.

#### CONCLUSIONS

Several important conclusions reached in this study are listed below.

- 1) Real-time X-ray radiography proved to be a nonintrusive, powerful and reliable tool for determining erosive-burning rates under confinement conditions.
- 2) The comprehensive erosive-burning model, based upon quasi-steady and 2-D axisymmetric mean-flow assumption, was validated by experimental data. The calculated time variation of internal diameter distribution along the grain agrees well with measured distributions.
- 3) The fine-wire thermocouple (5 to 25  $\mu\text{m}$  wire diameters) was incorporated into the erosive- and strand-burning investigations. The thermocouple can be used not only for measuring the temperature variation in the condensed phase, but also as a part of the gas-phase flame structure.
- 4) The erosive-burning augmentation factor was found to be very important during the early phase of the combustion processes in the center-perforated grain.
- 5) Three modes (fizz, unsteady flame, and steady flame) of gas-phase combustion processes were observed in strand-burning tests of NOSOL-363 propellants.

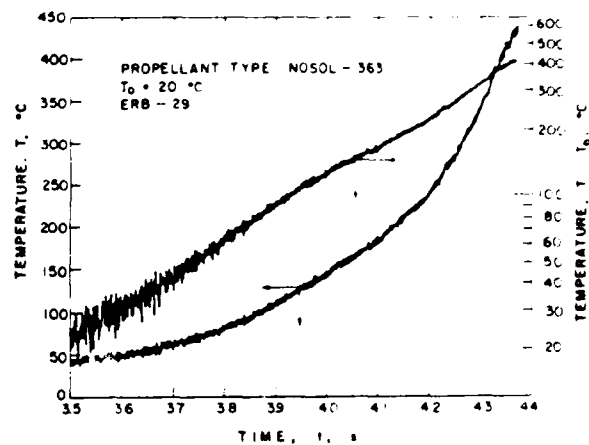


Fig. 18 The Temperature-Time Trace Obtained from an Erosive-Burning Test (ERB-29).

- 6) Two different sets of burning rate exponents and coefficients were deduced from burning rate data obtained from strand burner tests. The slope break point at  $P = 2.17$  MPa was found to be the boundary of unsteady and steady flame modes.
- 7) From temperature-time traces obtained in strand burning tests, burning surface temperatures were found to be a power law of pressure.
- 8) The activation energies for NOSOL-363 stick propellants are 8.13 kcal/mole in fizz and unsteady flame modes, and 14.7 kcal/mole in steady flame mode.
- 9) From numerical solutions, the erosive burning is found to be the result of enhanced heat feedback from the gas phase to solid propellant resulting from the combined effects of increased turbulent mixing and reduction in flame stand-off distance from the burning surface.

#### REFERENCES

1. Robbins, F. W. and Horst, A. W., "Continued Study of Stick Propellant Combustion Processes," ARBRL-MR-03296, July 1983.
2. Hsieh, Y. C. and Kuo, K. K., "Numerical Simulation of Combustion Processes of Mobile Stick-Propellant Bundles," 23rd JANNAF Combustion Meeting, Hampton, Va., October 1986.
3. Peters, S. T., "Selected Properties of Navy Gun Propellants," Indian Head Special Publication 84-194, February 1984.
4. Razdan, M. K. and Kuo, K. K., Fundamentals of Solid-Propellant Combustion, eds. Kuo, K. K. and Summerfield, M., Vol. 90, Progress in Astronautics and Aeronautics, Ch. 10, 1984.



END

10-87

DTIC